Electronic Supplementary Material (ESI) for Physical Chemistry Chemical Physics.

Supporting Information

Metallic Re_3O_2 with Mixed-Valence States

Wenjing Li[1], Fei Li[2,*], Xiaohua Zhang[2], Jinhui Wu[1] and Guochun Yang[1,2,*]

[1]*Centre for Advanced Optoelectronic Functional Materials Research and Key Laboratory for UV Light-Emitting Materials and Technology of Ministry of Education, Northeast Normal University, Changchun 130024, China*

[2]*State Key Laboratory of Metastable Materials Science & Technology and Key Laboratory for Microstructural Material Physics of Hebei Province, School of Science, Yanshan University, Qinhuangdao 066004, China*

*Corresponding Authors E-mail:yanggc468@nenu.edu.cn; yanggc@ysu.edu.cn

Index **Page**

Computational Details

The structure prediction method was based on a global minimization of free energy surfaces combining *ab initio* total-energy calculations methodology, as implemented in the CALYPSO (Crystal structure AnaLYsis by Particle Swarm Optimization) code.[1, 2] The structures of Re_xO_y (x = 1 y = 1-5; x = 2 y = 1, 3, 5, 7; x = 3 y = 1, 2) were searched with simulation cell sizes of 1-4 formula units (f.u.) at the selected pressures of 1 atm and 50, 100, 200, 300 GPa. In the first step, random structures with certain symmetry were constructed in which atomic coordinates were generated by the crystallographic symmetry operations. Local optimizations using the VASP code[3] were done with the conjugate gradients method and stopped when the total enthalpy changes became smaller than 1×10^{-5} eV per cell. After processing the first-generation structures, 60% of them with lower enthalpies were selected to construct the next generation structures by PSO (Particle Swarm Optimization). 40% of the structures in the new generation were randomly generated. A structure fingerprinting technique of bond characterization matrix was applied to the generated structures, so that identical structures are strictly forbidden. These procedures significantly enhanced the diversity of the structures, which was crucial for structural global search efficiency. In most cases, structural searching simulations for each calculation were stopped after generating 1000 ~ 1200 structures (e.g., about 20 ~ 30 generations).

To further analyze the structures with higher accuracy, we selected a number of structures with lower enthalpies and performed structural optimization using density functional theory within the generalized gradient approximation[4] as implemented in the VASP code. In all the calculations, the cutoff energy for the expansion of wavefunctions in plane waves was set to 750 eV, and the Monkhorst-Pack k-mesh with a grid spacing of $2\pi \times 0.03$ $Å^{-1}$ was selected to meet well energy convergence within ~1 meV/atom. The electron-ion interaction was described by the projector-augmented-wave potentials with $5d^5 6s^2$ and $2s^2 2p^4$ configurations considered as valence electrons for Re and O atoms, respectively.

In order to further test the reliability of the adopted pseudopotentials for Re and O, the validity of the projector augmented wave (PAW) pseudopotentials from the VASP library were checked by comparing the calculated Birch-Murnaghan equation of state with those obtained from the full-potential linearized augmented plane-wave method (LAPW, as implemented in WIEN2k).[5] The Birch-Murnaghan equation of states derived from PAW and LAPW methods were almost identical (Figure S0). Thus, our adopted pseudopotentials were feasible in the range of 0-300 GPa.

The electron-phonon coupling calculations were carried out with the density functional perturbation theory (DFPT) in the QUANTUM ESPRESSO package.[6] We employed the ultrasoft pseudopotentials with $5d^5 6s^2$and $2s^2 2p^4$ as valence electrons for Re, and O atoms, respectively. The kinetic energy cutoff and width of the Gaussians were chosen as 100 and 0.05 Ry. To reliably calculate electron-phonon coupling in metallic systems, we need to sample dense k-meshes for electronic Brillouin zone integration and enough q-meshes for evaluating average contributions from the phonon modes. Dependent on the specific structures of stable compounds, different k-meshes and q-meshes were used: 16 × 16 × 12 k-meshes and 4 ×4 × 3 q-meshes for ReO_4 in the $C2/m$ structure, 8 × 6 × 9 k-

meshes and 4 ×3 × 3 q-meshes for ReO_3 in the *Pnma* structure, 12 × 12 × 8 k-meshes and 4 × 4 × 4 q-meshes for ReO_2 in the *Cmca* structure, 15 × 15 × 2 k-meshes and 5 × 5 × 2 q-meshes for Re_3O_2 in the $P6_3/mmc$ structure. We have calculated the superconducting T_c of Re-O compounds as estimated from the McMillan-Allen-Dynes formula:[7-9]

$$T_c = \frac{\omega_{log}}{1.2} exp\left[-\frac{1.04(1 + \lambda)}{\lambda - \mu^*(1 + 0.62\lambda)} \right].$$

Here, μ^* is the Coulomb pseudopotential ($\mu^* = 0.1$). The electron-phonon coupling constant, λ, and the logarithmic average phonon frequency, ω_{log}, were calculated by the Eliashberg spectral function for electron-phonon interaction:

$$\alpha^2 F(\omega) = \frac{1}{N(E_F)} \sum_{kq,v} |g_{k,k+q,v}|^2 \delta(\varepsilon_k) \delta(\varepsilon_{k+q}) \delta(\omega - \omega_{q,v}),$$

where $\lambda = 2\int d\omega \frac{\alpha^2 F(\omega)}{\omega}$; $\omega_{log} = exp\left[\frac{2}{\lambda}\int \frac{d\omega}{\omega} \alpha^2 F(\omega) ln(\omega)\right]$. Herein, $N(E_F)$ is the electronic density of states at the Fermi level, $\omega_{q,v}$ is the phonon frequency of mode v and wave vector q, and $|g_{k,k+q,v}|$ is the electron-phonon matrix element between two electronic states with momenta k and $k + q$ at the Fermi level.[10, 11]

Supporting Figures

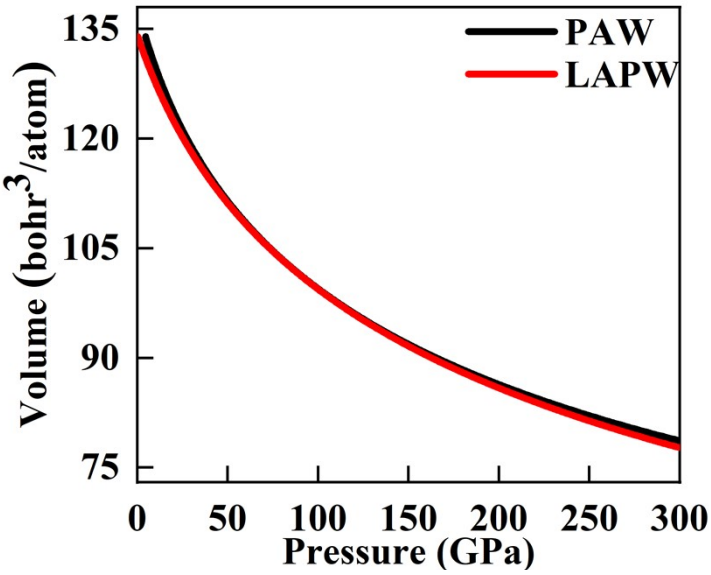

FIG. S0. Comparison of the fitted Birch-Murnaghan equation of states for *Cmcm*-ReO_4 by using the calculated results with the PAW pseudopotentials and the full-potential LAPW methods.

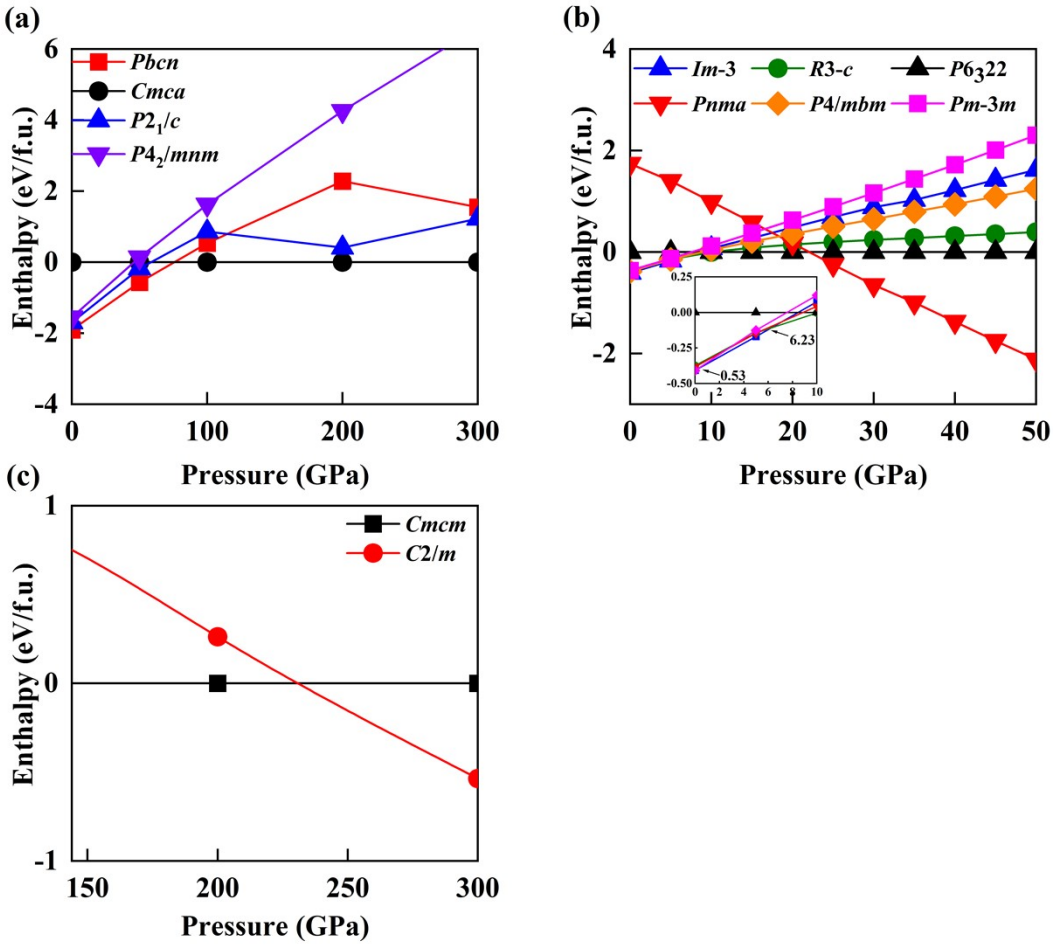

FIG. S1. Calculated enthalpy as a function of pressure for the reported and predicted (a) ReO_2, (b) ReO_3, and (c) ReO_4 phases.

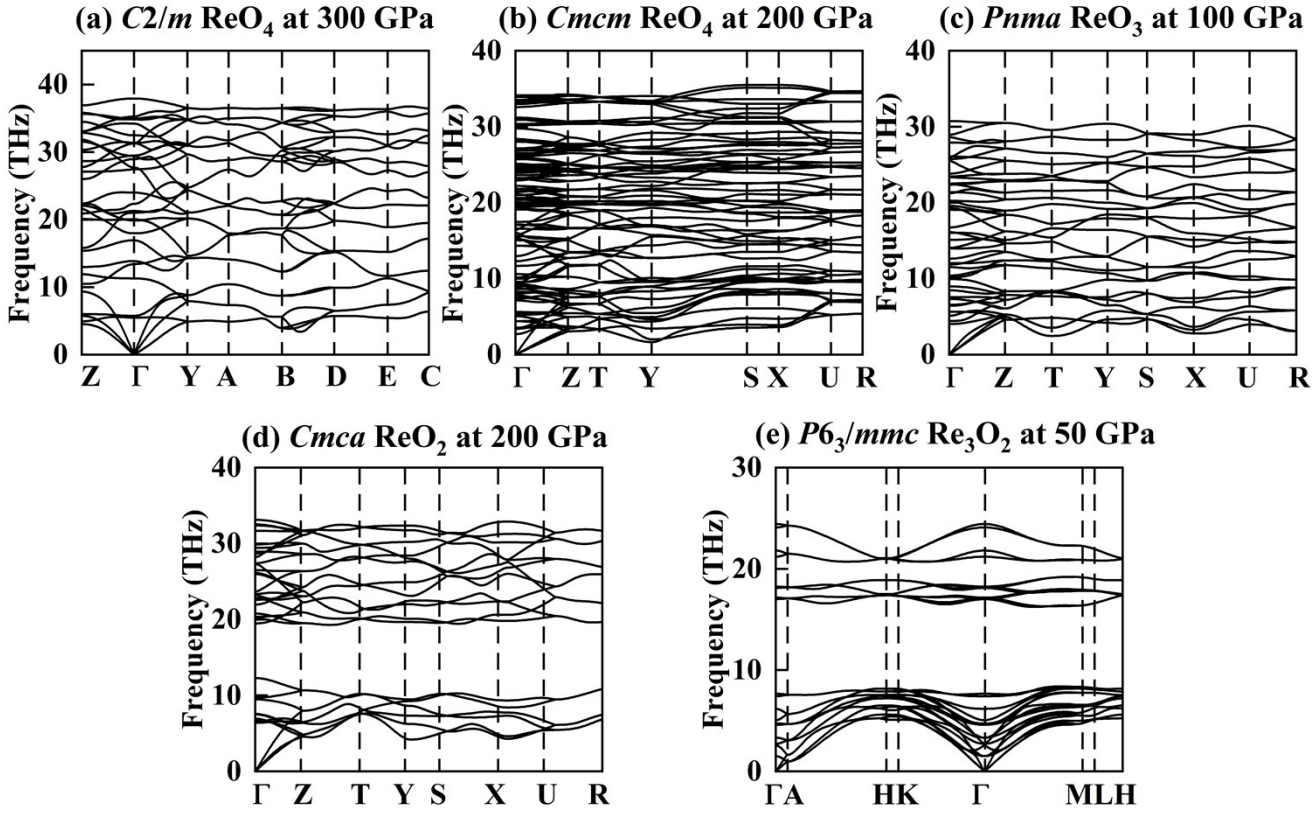

FIG. S2. Phonon dispersion curves of the stable Re-O phases.

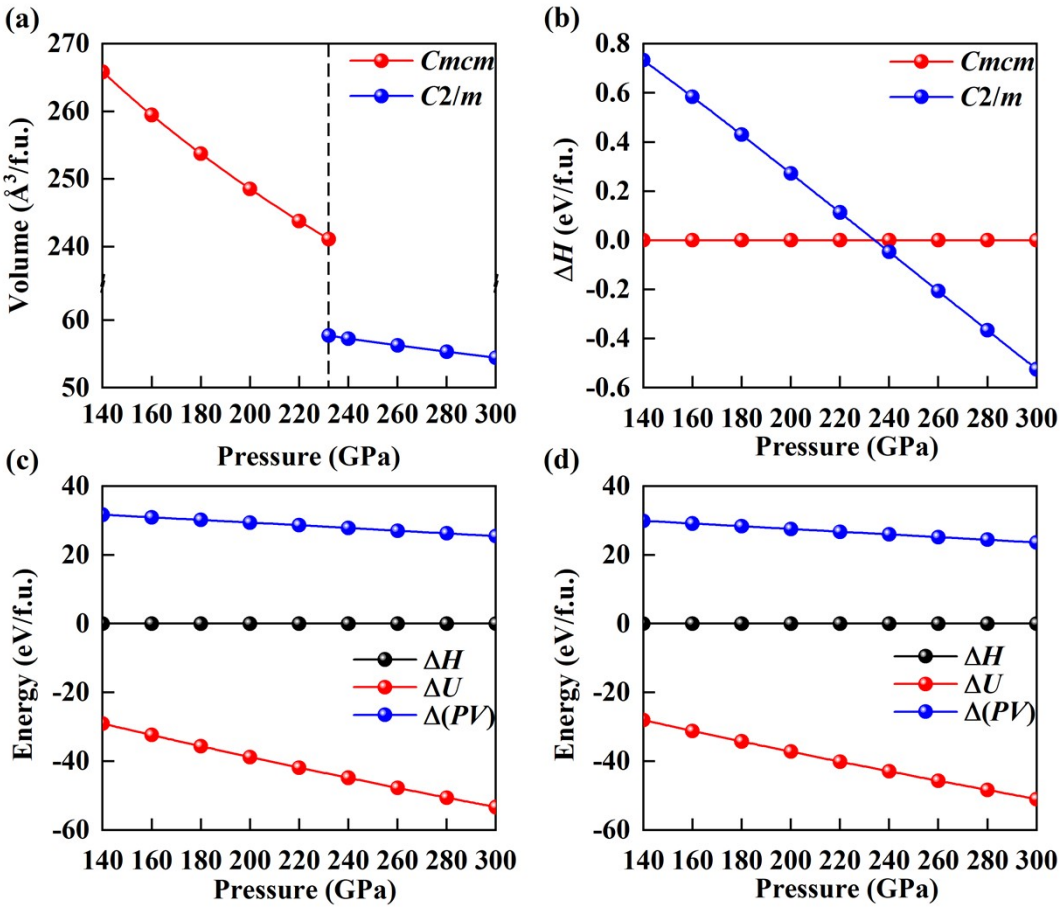

FIG. S3. The volume (a), the formation enthalpy (ΔH) (b), ΔH, ΔU, and $\Delta(PV)$ (c-d) as a function of pressure of *Cmcm* and *C*2/*m* ReO_4 within pressure range from 140 to 220 GPa.

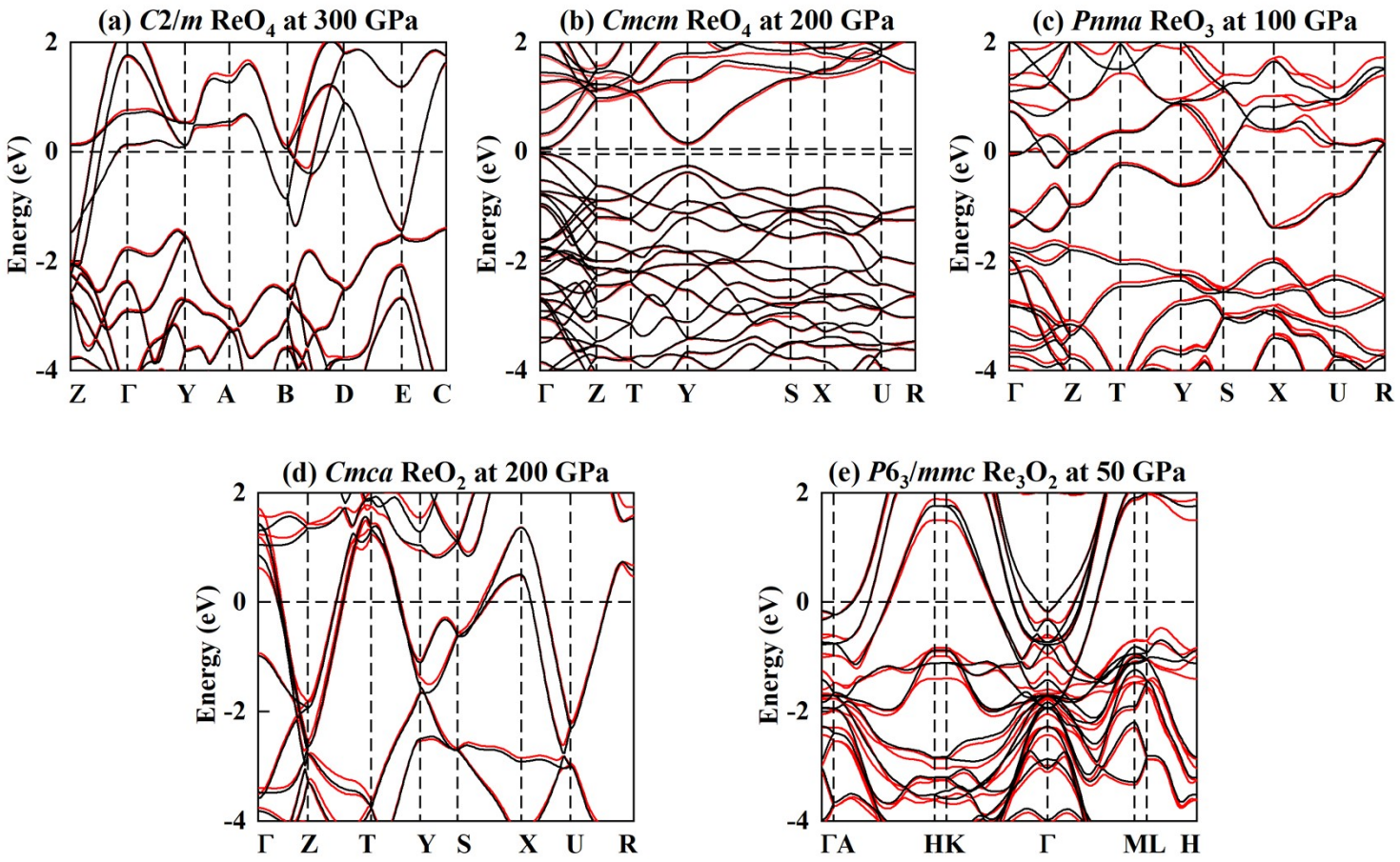

FIG. S4. Electronic band structures of the Re-O compounds (black line without SOC; red line with SOC).

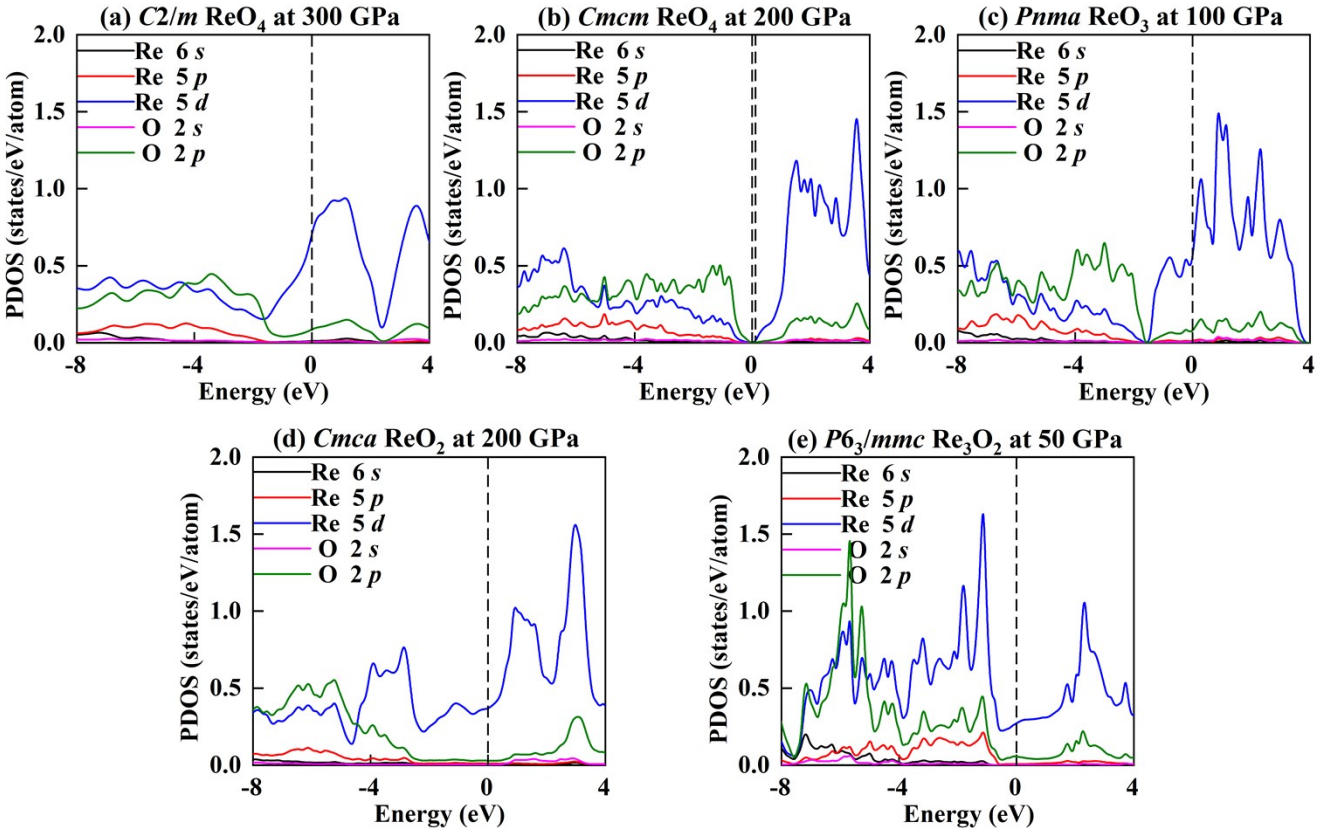

FIG. S5. PDOS of the Re-O compounds.

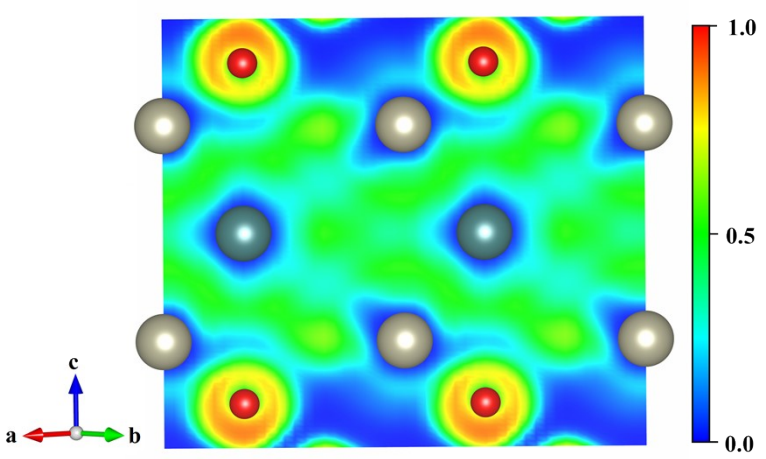

FIG. S6. Electron localization function of $P6_3/mmc$ Re_3O_2 at 50 GPa along (1 1 0) plane.

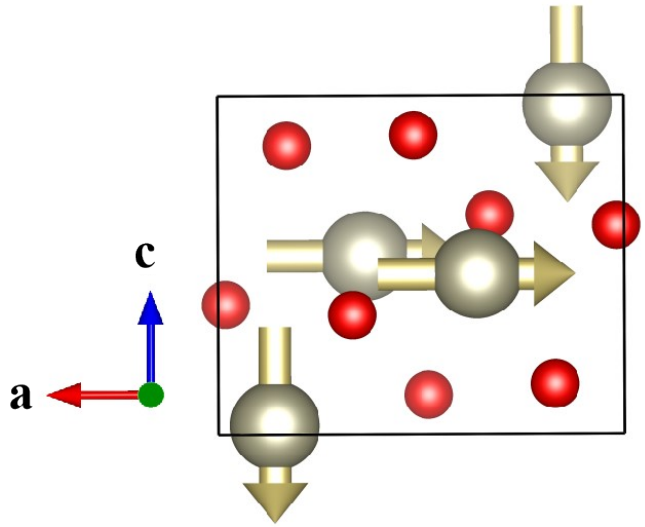

FIG. S7. Vibrational modes with lowest-frequency acoustic branch at T point of *Pnma*-ReO_3 at 100 GPa.

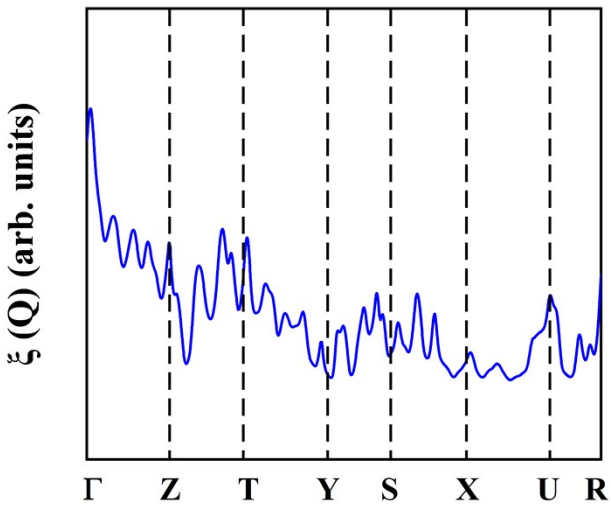

FIG. S8. Nesting function of *Pnma*-ReO_3 at 100 GPa.

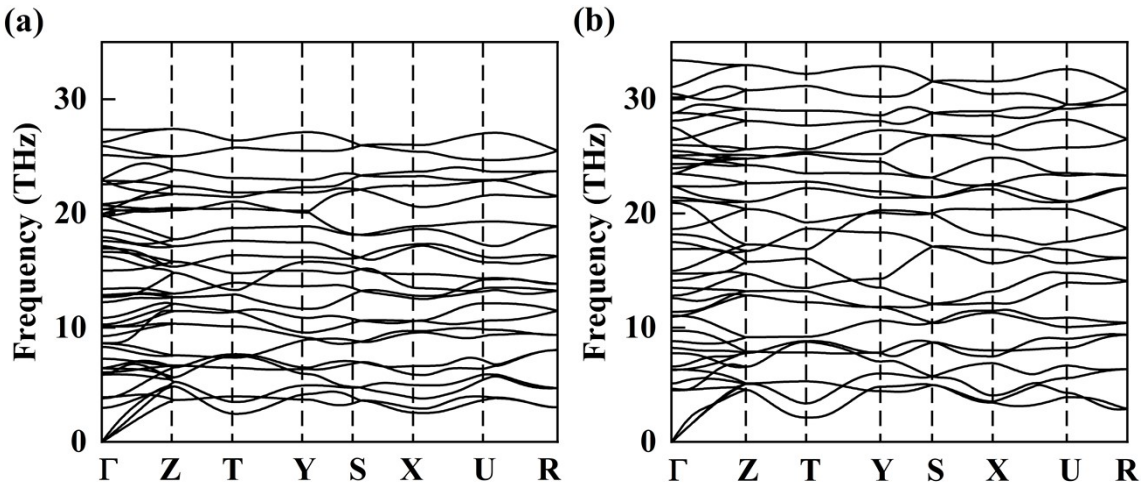

FIG. S9. Phonon dispersion curves of *Pnma*-ReO_3 at (a) 50 and (b) 150 GPa.

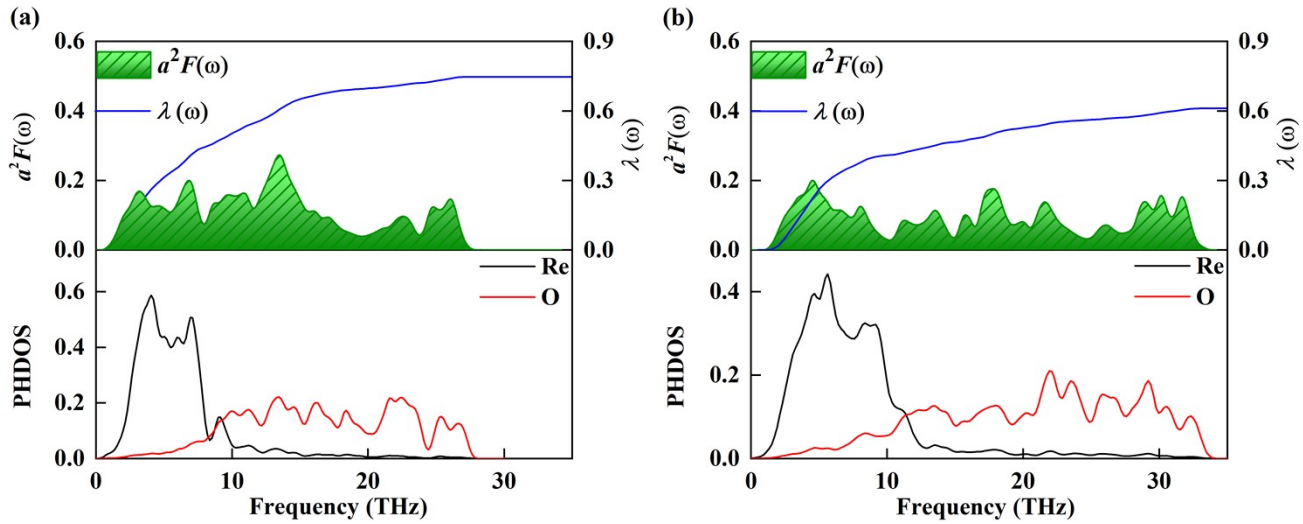

FIG. S10. The projected phonon densities of states (PHDOS) and Eliashberg spectral functions of *Pnma*-ReO_3 (a) 50 and (b) 150 GPa.

Supporting Tables

Table S1. Structural information of the predicted stable Re-O phases.

Phases	Pressure (GPa)	Lattice Parameters (Å, °)	Wyckoff Positions (fractional)			
			Atoms	*x*	*y*	*z*
***Cmca*-ReO_2**	200	a = 3.3255	Re(4b)	0.00000	0.50000	0.00000
		b = 5.6537	O(8f)	0.00000	0.16659	0.89847
		c = 4.2807				
		α = 90.0000				
		β = 90.0000				
		γ = 90.0000				
***Pnma*-ReO_3**	100	a= 4.9341	Re(4c)	0.63788	0.25000	0.52693
		b= 5.8198	O(8d)	0.33055	0.06349	0.64764
		c= 4.1312	O(4c)	0.48236	0.25000	0.11626
		α = 90.0000				
		β = 90.0000				
		γ = 90.0000				
***Cmcm*-ReO_4**	200	a = 10.7615	Re(8e)	0.63192	0.00000	0.50000
		b = 3.5631	O(8e)	0.81579	0.00000	0.50000
		c = 6.4855	O(8g)	0.70099	0.09777	0.25000
		α = 90.0000	O(8g)	0.06177	0.21846	0.25000
		β = 90.0000	O(8f)	0.00000	0.23703	0.90629
		γ = 90.0000				
***C*2/*m*-ReO_4**	300	a = 5.4832	Re(2d)	0.00000	0.50000	0.50000
		b = 3.1122	O(4i)	0.86351	0.50000	0.96057
		c = 4.3216	O(4i)	0.91123	0.00000	0.66437
		α = 90.0000				
		β = 132.3880				
		γ = 90.0000				
***P*6_3/*mmc*-Re_3O_2**	50	a = 2.7108	Re(2d)	0.66667	0.33333	0.25000
		b = 2.7108	Re(4e)	0.00000	0.00000	0.87577
		c = 16.8541	O(4f)	0.33333	0.66667	0.94845
		α = 90.0000				
		β = 90.0000				
		γ = 120.0000				

Table S2. The integrated PDOS value of Re_3O_2 phases at 50 GPa.

Phases	Pressure (GPa)	Atoms	IPDOS
***P*6$_3$/*mmc*-Re$_3$O$_2$**	0	Re_I-*s*	0.67
		Re_I-*p*	0.81
		Re_I-*d*	5.13
		Re_{II}-*s*	0.62
		Re_{II}-*p*	0.89
		Re_{II}-*d*	5.04
		O-*s*	1.59
		O-*p*	3.47

Table S3. Bader charge transfer amount of Re and O atoms in the Re_3O_2 phases at 50 GPa.

Phases	Pressure (GPa)	Atoms	Charge(e)
***P*6$_3$/*mmc*-Re$_3$O$_2$**	50	Re_I	0.02
		Re_{II}	0.88
		O	-0.89

Table S4. Bader charge transfer amount of Re and O atoms in ReO_3 phases at 50-150 GPa.

Phases	Pressure (GPa)	Atoms	Charge(e)
***Pnma*-ReO$_3$**	50	Re1	2.56
		O1	-0.88
		O2	-0.81
***Pnma*-ReO$_3$**	100	Re1	2.61
		O1	-0.89
		O2	-0.83
***Pnma*-ReO$_3$**	150	Re1	2.65
		O1	-0.90
		O2	-0.85

Table S5. Superconducting properties of the metallic Re-O phases.

Phases	Pressure (GPa)	λ	ω_{log} (K)	N_{Ef}	T_c (K)
***Pnma*-ReO_3**	50	0.74	297.64	32.82	11.90
***Pnma*-ReO_3**	100	0.87	210.81	28.07	11.52
***Pnma*-ReO_3**	150	0.61	333.82	25.55	8.07
***Cmca*-ReO_2**	200	0.21	423.22	6.79	0.01
***C*2/*m*-ReO_4**	300	0.28	549.89	6.89	0.12
***P*6$_3$/*mmc*-Re_3O_2**	0	0.31	224.25	16.31	0.17
***P*6$_3$/*mmc*-Re_3O_2**	50	0.25	278.49	14.37	0.02

References

1. Y. Wang, J. Lv, L. Zhu and Y. Ma, *Phys. Rev. B*, 2010, **82**, 094116.
2. Y. Wang, J. Lv, L. Zhu and Y. Ma, *Comput. Phys. Commun.*, 2012, **183**, 2063-2070.
3. G. Kresse and J. Furthmüller, *Phys. Rev. B*, 1996, **54**, 11169-11186.
4. J. P. Perdew, J. A. Chevary, S. H. Vosko, K. A. Jackson, M. R. Pederson, D. J. Singh and C. Fiolhais, *Phys. Rev. B*, 1992, **46**, 6671-6687.
5. P. Blaha, K. Schwarz, P. Sorantin and S. B. Trickey, *Comput. Phys. Commun.*, 1990, **59**, 399-415.
6. P. Giannozzi, S. Baroni, N. Bonini, M. Calandra, R. Car, C. Cavazzoni, D. Ceresoli, G. L. Chiarotti, M. Cococcioni, I. Dabo, A. Dal Corso, S. de Gironcoli, S. Fabris, G. Fratesi, R. Gebauer, U. Gerstmann, C. Gougoussis, A. Kokalj, M. Lazzeri, L. Martin-Samos, N. Marzari, F. Mauri, R. Mazzarello, S. Paolini, A. Pasquarello, L. Paulatto, C. Sbraccia, S. Scandolo, G. Sclauzero, A. P. Seitsonen, A. Smogunov, P. Umari and R. M. Wentzcovitch, *J. Phys.: Condens. Matter*, 2009, **21**, 395502.
7. L. N. Oliveira, E. K. U. Gross and W. Kohn, *Phys. Rev. Lett.*, 1988, **60**, 2430-2433.
8. M. Lüders, M. A. L. Marques, N. N. Lathiotakis, A. Floris, G. Profeta, L. Fast, A. Continenza, S. Massidda and E. K. U. Gross, *Phys. Rev. B*, 2005, **72**, 024545.
9. M. A. L. Marques, M. Lüders, N. N. Lathiotakis, G. Profeta, A. Floris, L. Fast, A. Continenza, E. K. U. Gross and S. Massidda, *Phys. Rev. B*, 2005, **72**, 024546.
10. P. B. Allen and B. Mitrovic, *Solid State Phys.*, 1982, **37**, 1-92.
11. J. P. Carbotte, *Rev. Mod. Phys.*, 1990, **62**, 1027-1157.